Journal of Geophysical Research: Earth Surface

RESEARCH ARTICLE
10.1029/2018JF004742

Quantifying Bed Level Change at the Transition of Tidal Flat and Salt Marsh: Can We Understand the Lateral Location of the Marsh Edge?

P. W. J. M. Willemsen[1,2,3], B. W. Borsje[1], S. J. M. H. Hulscher[1], D. Van der Wal[2,4], Z. Zhu[2], B. Oteman[2], B. Evans[5], I. Möller[5], and T. J. Bouma[2]

[1]Water Engineering and Management, University of Twente, Enschede, The Netherlands, [2]Department of Estuarine and Delta Systems, NIOZ Royal Netherlands Institute for Sea Research and Utrecht University, Yerseke, The Netherlands, [3]Department of Ecosystems and Sediment Dynamics, Deltares, Delft, The Netherlands, [4]Faculty of Geo-Information Science and Earth Observation (ITC), University of Twente, Enschede, The Netherlands, [5]Cambridge Coastal Research Unit, Department of Geography, University of Cambridge, Cambridge, UK

Key Points:
- Biophysical interactions determine bed level change, both at the salt marsh and tidal flat
- Bed level change and inundation time control the lateral position of the marsh edge by driving vegetation growth
- For vegetation to withstand longer inundation requires stable bed levels while; withstanding dynamic bed levels requires less inundation

Correspondence to:
P. W. J. M. Willemsen,
p.willemsen@utwente.nl

Citation:
Willemsen, P. W. J. M., Borsje, B. W., Hulscher, S. J. M. H., Van der Wal, D., Zhu, Z., Oteman, B., et al. (2018). Quantifying bed level change at the transition of tidal flat and salt marsh: Can we understand the lateral location of the marsh edge? *Journal of Geophysical Research: Earth Surface*, *123*, 2509–2524. https://doi.org/10.1029/2018JF004742

Received 4 MAY 2018
Accepted 15 SEP 2018
Accepted article online 19 SEP 2018
Published online 22 OCT 2018

Abstract Bed level dynamics at the interface of the salt marsh and tidal flat have been highlighted as a key factor connecting the long-term biogeomorphological development of the marsh to large-scale physical forcing. Hence, we aim to obtain insight into the factors confining the location of the marsh edge (i.e., boundary between tidal flat and salt marsh). A unique data set was collected, containing measurements of daily bed level changes (i.e., integrative result of physical forcing and sediment properties) at six intertidal transects in the North Sea area. Moreover, various biophysical parameters were measured, such as sediment characteristics, waves, inundation time, and chlorophyll-*a* levels. The data show that both bed level change and waves decreased from the lower intertidal flat toward the marsh edge and further diminished inside the marsh. However, no direct general relation was found between waves and bed level change. Bed level change inside the marsh was always small, regardless of wave energy. By combining the data sets, we demonstrate that the location of the lower marsh edge is restricted by two interacting factors: inundation time and bed level change. For vegetation establishment to withstand longer inundation stress, which slows down plant growth, more stable bed levels are required so that plants are not heavily disturbed. Conversely, to withstand more dynamic bed levels that disturbs plant growth, lower inundation stress is needed, so that plants grow fast enough to recover from the stress. The results suggest that bed level change is important in determining the position of the marsh edge.

1. Introduction

Tidal flats and salt marshes are widespread coevolving ecosystems in the coastal region (Marani et al., 2007; Mcowen et al., 2017). They provide multiple ecosystem services like carbon sequestration (Chmura et al., 2003; Duarte et al., 2013), filtering water (Nelson & Zavaleta, 2012), providing a habitat and nursery ground (Irmler et al., 2002; Van Eerden et al., 2005), and improving coastal safety by stabilizing the bed and attenuating waves (Temmerman et al., 2013; Vuik et al., 2016). Especially the protective value of salt marshes by attenuating waves even under extreme conditions has been increasingly recognized in recent years (Barbier et al., 2008; Gedan et al., 2011; Moller et al., 2014; Shepard et al., 2011). This protective value benefits from salt marshes being able to counteract both sea level rise and land subsidence by sediment accretion (Kirwan et al., 2016). However, it has been noted that large-scale application of salt marshes for coastal defense requires in-depth understanding of their long-term lateral dynamics and persistence (Borsje et al., 2011; Bouma et al., 2014).

Lateral dynamics determine the cross-shore location of the marsh edge and thereby the width of a salt marsh. In many locations, the marsh edge shifts up to several meters per year and is known to show cyclic alternations between erosion and expansion on a decadal or longer time scale (Allen, 2000; Singh Chauhan, 2009; Van der Wal et al., 2008). The switch between these two phases is determined by two key processes: initiation of marsh erosion (i.e., start of retreat) and start of expansion by seedling establishment (Bouma et al., 2016) and growth of clonal shoots (Silinski et al., 2016). Whereas the rate of marsh erosion is determined by frequent flooding and wave events (Fagherazzi, 2014; Wang et al., 2017), the onset of erosion may originate

from a discontinuity by having a stable marsh platform level adjacent to a dynamic tidal flat, where the bed level can vary greatly over time (Bouma et al., 2016). The process of seedling establishment at the tidal flat is mainly affected by the physical parameters: relative elevation in the tidal frame, which determines the inundation frequency and period (Balke et al., 2016); and bed level change, which possibly lead to uprooting and/or burying seedlings (Hu, van Belzen, et al., 2015). Clonal expansion is mainly affected by hydrodynamic conditions (i.e., inundation period and hydrodynamic energy) at the tidal flat (Silinski et al., 2016). This raises the question as to whether the location of the marsh edge may be determined by both the bed level change and inundation period at the tidal flat fronting the marsh edge.

Bed level change is an interesting parameter in that it integrates a suite of physical and biological processes on the tidal flat and salt marsh that potentially influence lateral dynamics: wave and/or tidal forcing exerting bed shear stresses (Friedrichs, 2011; Green & Coco, 2014; Hu et al., 2017; Hunt et al., 2015), grain size properties determining the critical erosion threshold (Deegan et al., 2012; Grabowski et al., 2011), bioturbation and bioaggregation (seasonally) modifying the critical erosion threshold of the bed (Andersen et al., 2005; Corenblit et al., 2011; Murray et al., 2008), and external sediment supply controlling sedimentation rates (Hu, Wang, et al., 2015; Mariotti & Fagherazzi, 2010; Willemsen et al., 2016). By affecting both salt marsh expansion and retreat, short-term bed level dynamics (i.e., seasonal and shorter changes in sediment elevation or bed level) at the tidal flat in front of a marsh have been indicated as the driving mechanism connecting long-term cyclic behavior of the marsh to large-scale physical forcing (Bouma et al., 2016). However, to date, only very few measurements of the short-term bed level dynamics exist near the tidal flat—salt marsh transition. Previous studies have mainly focused on the occurrence of seasonality in sedimentation and erosion (e.g., Herman et al., 2001) and in hydrodynamic forcing (Callaghan et al., 2010). Hence, in this paper we aim to quantify the bed level change at the marsh edge across a number of contrasting locations and over a daily to annual time scale.

Whereas long-term bed level dynamics, that is, accretion and erosion of the top tens of centimeters of the bed, have been studied extensively using a suite of methods with a temporal resolution of weeks to months (e.g., erosion pins (Stokes et al., 2010), a steel reference plate (Andersen et al., 2006) and accretion poles (O'Brien et al., 2000), methods for monitoring daily bed level changes, such as the Photo-Electronic Erosion Pin (PEEP) system (Lawler, 2008) remain rarely applied due to high costs (for review see Hu, Lenting, et al., 2015). The Surface Elevation Dynamic (SED) sensor was developed and tested as affordable way to collect long-term measurements of daily bed level change. Hu, Lenting, et al. (2015) showed the principle, accuracy, and application of these sensors for understanding the morphodynamics of tidal flats.

To obtain a better understanding of the factors constraining the location of the marsh edge at any particular point in time and to ascertain whether bed level change and inundation period may be important in this, we (i) deployed SED sensors at the transition between salt marsh and tidal flat for a range of contrasting locations and (ii) coupled these SED measurements to a range of biophysical parameters such as sediment characteristics, wind waves, inundation time, and chlorophyll-*a* levels of the sediment (as a proxy for the presence of microphytobenthos biomass).

2. Materials and Methods

2.1. Study Sites

The study sites are situated around the North Sea, with sites in the Westerschelde, Wadden Sea and Thames estuary (Figure 1) and comprise measurements from different field studies. The four main study sites are located in the Westerschelde. The Westerschelde estuary (51°20′N; 4°E; Figure 1) is located in the southwestern delta of the Netherlands (Figure 1). The estuary is mesotidal to macrotidal and is tide dominated, having a semidiurnal tide (Baeyens et al., 1997). Salinity at the mouth of the Westerschelde (near Vlissingen) is around 25 practical salinity unit (psu) and around 10 psu at the Dutch-Belgian border, increasing during summer and decreasing during winter (Damme et al., 2005). The prevailing wind direction in the Westerschelde estuary is southwest, measured by the KNMI (Royal Netherlands Meteorological Institute) at Hansweert (Figure 1). The sites at the northern shore are exposed, and the sites at the southern shore are more sheltered from the prevailing wind (Callaghan et al., 2010). Four sites in the Westerschelde were studied, two at the northern shore at approximately 20 and 50 km from the mouth and two at the southern shore at approximately 15 and 27 km from the mouth (Figure 1 and Table 1). The two most westerly study sites were

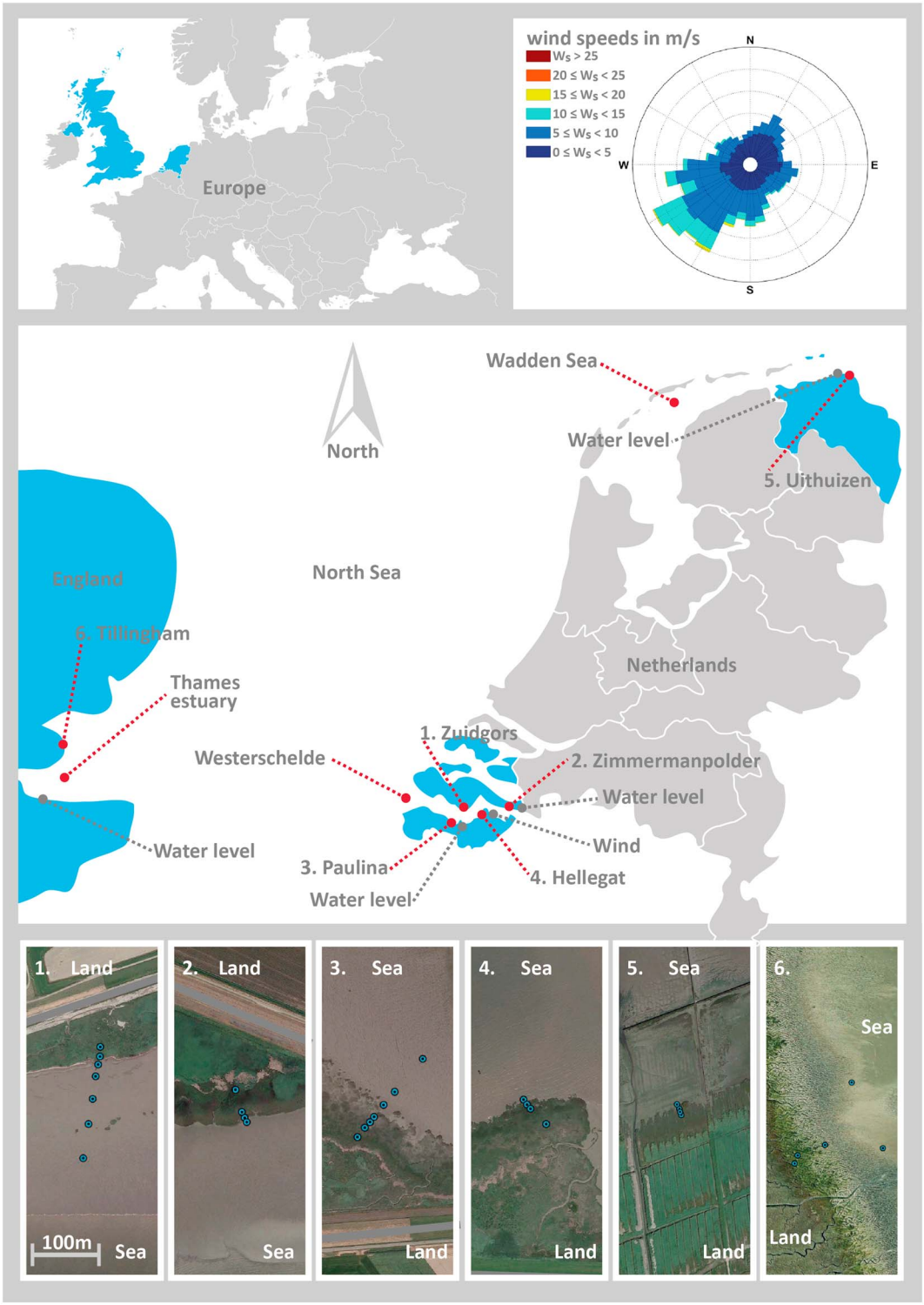

Figure 1. Location and overview of the study sites in the Westerschelde and Wadden Sea in the Netherlands, and the Thames Estuary in England (Europe) including wind speeds measured by the KNMI (Royal Netherlands Meteorological Institute; top right panel). Two sites in the Westerschelde are located at the most wind exposed northern shore sites (1E. Zuidgors and 2E. Zimmermanpolder) and two sites at the more sheltered southern shore (3S. Paulina and 4S. Hellegat). The fifth and sixth sites are located in the Wadden Sea (5.Uithuizen) and Thames estuary (6. Tillingham), respectively. (source aerial imagery: Google earth).

Table 1
Locations of the Study Sites and Periods in Which Bed Level Data Were Collected at the Study Sites

Study site	Location	Start data collection	End data collection	Locations relative to marsh edge (negative is landward; m)
1E. Zuidgors	51°23′21.95″N, 3°50′7.51″E; Westerschelde	October 2015	October 2016	−20; −5; 5; 25; 60; 100; 155
2E. Zimmerman-polder	51°24′8.05″N, 4°10′32.15″E; Westerschelde	February 2015	June 2016	−50; −15; −5; 5
3S. Paulina	51°20′59.73″N, 3°43′3.37″E; Westerschelde	February 2015	June 2016	−42.5; −25.5; −17.5; −2.5; 22.5; 47.5; 127.5
4S. Hellegat	51°21′59.33″N, 3°56′44.67″E; Westerschelde	December 2014	August 2016	−50; −15; −5; 5
5. Uithuizen	53°27′24.57″N, 6°39′32.07″E; Wadden Sea	March 2015	March 2016	−15; −10; −5; 2.5
6. Tillingham	51°41′40.37″N, 0°56′32.80″E; Thames Estuary	July 2015	July 2016	−5; 7.5; 52.5; 125; 130

saline during the most recent measurements (approximately 20–25 psu), while the eastern study sites were mostly brackish (approximately 15–20 psu) (Damme et al., 2005). The field sites in the Westerschelde were 1E. Zuidgors, 2E. Zimmermanpolder, 3*S. Paulina* and 4S. Hellegat, with *E* indicating exposed and *S* indicating sheltered from the prevailing wind (Figure 1). The spring tidal range increases from approximately 4.4 m at the most westerly study site to 5.5 m at the most easterly study site (Van der Wal et al., 2008). Pioneer species occurring at the different study sites are mainly perennial common cord grass (*Spartina anglica*) and the annual glasswort (*Salicornia spp*.). Common saltmarsh grass (*Puccinellia maritima*), annual seablite (*Suaeda maritima*), and sea aster (*Aster tripolium*) vegetation occurs higher in the marsh. The most eastern marsh (upstream), 2E. Zimmermanpolder, has a more brackish environment. Seaside bulrush (*Bolboschoenus maritimus*) and common reed (*Phragmatis australis*), occurs apart from *Spartina spp*. (Van der Wal et al., 2008).

To generalize physical mechanisms driving marsh edge dynamics and to validate the results obtained in the Westerschelde, bed level change of the Wadden Sea (5. Uithuizen) and Thames estuary (6. Tillingham) was studied accordingly. The Wadden sea is a mesotidal to macrotidal estuary (Dieckmann et al., 1987), with a tidal range of about 4.0 m near the study site. Pioneer vegetation species occurring at study site 5. (Uithuizen), are common glasswort (*Salicornia europaea*), common salt marsh grass (*Puccinellia maritima*), and common cordgrass (*Spartina anglica*). The landward occurring more mature plant species are couch grass (*Elymus athericus*), sea aster (*Aster tripolium*), and seepweed (*Suaeda maritima*). The Thames estuary is macrotidal, with a tidal range of about 4.8 m near the study site (Reed, 1988). Vegetation species occurring at study site 6. Tillingham include pioneer species like common saltmarsh-grass (*Puccinellia maritima*), common cordgrass (*Spartina*), and common glasswort (*Salicornia*), and higher marsh species like sea purslane (*Atriplex portulacoides*), sea aster (*Aster tripolium*), and couch grass (*Elymus athericus*) (Rupprecht et al., 2015).

2.2. Field Data Collection and Laboratory Analysis: Bed Level Change, Sediment Characteristics, Waves, Inundation Time, and Microphytobenthos

Bed level changes were collected at all six study sites at the interface of the tidal flat and salt marsh (Figure 1; bottom panels), using the recently developed SED sensors (Hu, Lenting, et al., 2015; Hu et al., 2017). The data were collected over a period of 2 years (Table 1). The stand-alone SED sensor was developed to continuously obtain high resolution temporal bed level data. The measuring section of the SED sensor consists of 200 adjacent light sensitive cells (i.e., phototransistors) of 2-mm height, resulting in a measurement domain of 400 mm. The total length of the instrument is 1,100 mm, with a cylinder of 510 mm below the measuring section. When installing the SED sensor in the field, half of the measuring section was below the bed level and the other half was above the bed level. The instrument was installed firmly in the sediment, since the total length below the bed level was approximately 700 mm. Bed level measurements were taken every 30 min. The SED sensor has previously been used to obtain bed level dynamics at a tidal flat (Hu, Lenting, et al., 2015). Both at location 1E. Zuidgors and 3*S. Paulina*, seven SED sensors were installed (Figure 1): at 1E. Zuidgors five instruments were installed in the tidal flat and two in the salt marsh and at 3*S. Paulina* three instruments were installed in the tidal flat and four in the salt marsh (Table 1). At location 2E. Zimmermanpolder and 4S. Hellegat four sensors were installed (Figure 1): three in the salt marsh and one in the tidal flat (Table 1). The SED sensors were installed at transects oriented approximately perpendicular to the salt marsh edge. At location 5. Uithuizen, four instruments were installed: one on the tidal flat and three on the salt marsh, while at location 6. Tillingham five instruments were installed: four on the tidal flat and one

on the salt marsh (Table 1 and Figure 1). The sensors closest to the vegetated marsh margin were installed within a minimum distance of 2.5 m and maximum distance of 7.5 m from the vegetation edge, to ensure measured bed level changes captured the marsh or tidal flat over the entire measurement period irrespective of marsh edge movements. The initial elevation of the transects was measured using an RTK-GPS device with a precision in the order of 1 cm.

Erosion pins were used to record bimonthly changes of the local surface level. The erosion pin is a very thin metal rod (i.e., to prevent scouring) with a height marker on top, and a ring around the pin. The pin was pushed into the sediment, with the marker at a fixed height above the sediment. A metal ring was placed around the pin on top of the soil surface. Every 2 months (bimonthly), bed level change was measured. The distance from the marker to the soil surface and the ring buried into the sediment were measured. After each measurement, the erosion pins were reinstalled at least 10 cm from their original position to prevent disturbance from the earlier measurements. Three pins were deployed per SED sensor location.

Sediment samples were collected from the upper 3 cm of the surface with a cut-off syringe at all measurement locations (near the SED sensors) of the study sites in the Westerschelde. The sediment samples were freeze dried in the laboratory, and the average grain size diameter (D50) of the sediment was determined using a Malvern laser particle sizer.

Wave measurements were conducted at field sites 2E. Zimmermanpolder and 4S. Hellegat. At both marshes, a wave gauge (Ocean Sensor Systems, Inc., United States) was located near every SED sensor, eight wave gauges in total. The pressure sensor of the wave gauges was installed approximately 0.10 m above the bed. Pressure was measured by the wave gauges with a frequency of 5 Hz over a period of 7 min, every 15 min. The local atmospheric pressure, hydrostatic pressure, and the dynamic wave pressure included in the measured signal were separated during postprocessing (Vuik et al., 2016). The dynamic wave pressure was used for determining the significant wave height (Hm0), derived from the wave spectrum. A continuous pressure signal was not present at all study sites, so for determining the inundation time, data were used from Rijkswaterstaat (Dutch department of waterways and public works), for consistency at all five Dutch study sites. The data were obtained at Terneuzen, Bath and Uithuizerwad (Figure 1; indicated by water level). Processed water level data at the measurement locations were available every 10 min. Water level data for Tillingham (England) were used from the British Oceanographic Data Centre. The data were obtained at the South side of the Thames estuary, at Sheerness, and were available every 15 min.

The bed of intertidal areas can be stabilized by diatoms (Andersen et al., 2005; Austen et al., 1999). An indicator for the biomass of this microphytobenthos at the intertidal area and the biostabilization is the chlorophyll-*a* level of the sediment (Andersen, 2001; Staats et al., 2001). The chlorophyll-*a* level of the sediment was measured bimonthly from November 2015 to July 2016 at 1E. Zuidgors. Chlorophyll-*a* samples were collected of the upper 1 cm of the sediment, using a small cut-off syringe. Samples were taken at each SED sensor. Around each sensor, six replicate samples were taken and merged into one sample. After storage at −80 °C for at least 1 day, they were freeze dried (at −20 °C) in a dark room for 72 hr and then brought to the −80 deg C freezer again for storage prior to further analysis in the laboratory. The samples were homogenized and photosynthetic pigments of a subsample were extracted using a cell homogenizer after addition of 10-ml acetone (90%) and glass beads. The extract was centrifuged and absorption was measured with a spectrophotometer.

2.3. Field Data Analysis

The bed level change at the different measurement locations were obtained by converting the raw data from the SED sensors to bed level change information (Appendix A), setting the first obtained measurement equal to zero and referring all other bed level measurements to this first point. The maximum positive and negative change per measurement location were selected for determining the amplitude of the bed level change over the entire measurement period. The amplitude of the bed level change per measurement location was seasonally aggregated, for spring (March–May), summer (June–August), fall (September–November), and winter (December–February). The maximum positive and negative change were selected, because this is an important parameter for seedling establishment in the appropriate season (i.e., once a threshold for erosion or sedimentation is exceeded seedlings will not be able to establish, Bouma et al., 2016).

Bed level measurements by SED sensors were validated using erosion pin measurements at 1E. Zuidgors. Erosion pins have been commonly used for measuring bed level change in coastal and fluvial areas and

are widely applied (e.g., Arens et al., 2004; Sirvent et al., 1997). The three measurement pins per SED sensor were averaged, and the standard deviation was determined. The bed level change measured with the SED sensors was compared with bed level change measured with erosion pins.

The maximum significant wave height (Hm0) was determined per tidal inundation, using the wave gauges at 2E. Zimmermanpolder and 4S. Hellegat. Assuming bed level changes are the result of a previous inundation, the maximum significant wave height from inundations after which bed level changes were obtained was taken into account only. So tidal inundations without subsequently measured bed levels were not used for analysis. For each selected tidal inundation the maximum significant wave height was obtained and all values were averaged per season per measurement location. Water level data obtained from the Rijkswaterstaat measurement locations (Figure 1) were compared with the bed level height of all measurement locations, since wave gauges were only located at two study sites. The periods of inundation were initiated once the water level exceeded the bed level at the measurement location and stopped when the water level was below the bed level again. Only tidal inundations after which bed level change was obtained were taken into account. The inundation period was averaged per season as well as per measurement location.

3. Results

3.1. Quantifying Daily Bed Level Change Across Seasons at the Salt Marsh-Tidal Flat Interface

The bed level change near the vegetation edge, both on the marsh and tidal flat, was observed with SED sensors at all study sites. The observations at 1E. Zuidgors in the Westerschelde, the Netherlands, revealed that the largest bed level change occurred at the most seaward measurement locations (bottom panels, Figure 2) and that the bed level change decreased toward the vegetated marsh (top panels, Figure 2). Measurements obtained by the SED sensor were comparable with the measurements obtained by the erosion pins (Figure 2; red bars), having a correlation (R^2) of 0.74, without a systematic deviation. The standard deviation over the three erosion pin measurements, per measurement location, was highest at the most seaward measurement locations during the spring and summer season (Figure 2). The much higher temporal resolution of the SED sensors allowed the identification of the exact timing of changes and calculation of the variability in bed level between pin readings (e.g., as standard deviation).

The largest positive seasonally aggregated bed level change (sedimentation) was observed in the spring and summer season (March–May; Figure 3) and was most pronounced on the tidal flat of the wind-exposed northern shores, that is, 1E. Zuidgors and 2E. Zimmermanpolder (Figures 3a and 3b, respectively). The spring sedimentation reversed during the summer (June–August), followed by maximum negative bed level change (erosion) during fall (September–November) and winter (December–February; Figure 3). A relatively stable bed level was observed at the locations landward from the marsh edge at 1E. Zuidgors, while more dynamic behavior was observed at the gradually changing profile of 2E. Zimmermanpolder (Figures 3a and 3b). The pattern of seasonal variation was less pronounced at the sheltered sites (Figures 3c and 3d, respectively). However, in general a clear distinction was observed between bed level change at the tidal flat (relative large) and salt marsh (relative small).

The largest amplitude of the bed level change over the entire measurement period (derived from the seasonal amplitude) at 1E. Zuidgors revealed that dynamics were larger further seaward and decreased in a landward direction toward the marsh (Figure 4). At all transects, the largest bed level change was observed at the most seaward measurement location (Figure 4). In general, the bed level change landward from the marsh edge remained smaller than the bed level change seaward from the marsh edge at all locations. Only the bed level change very near to the marsh edge, just inside the pioneer vegetation and just landward of the marsh edge (i.e., within a range of 10 m) at the wind exposed sites (Figure 4; sites 1 and 2) did not comply with the landward decreasing trend in bed level change. In general, these results clearly show that bed level change decreases (i.e., sediment stability increases) in the presence of vegetation. When comparing exposed versus sheltered sites, the most pronounced bed level change was observed at the exposed northern shores.

3.2. Bed Level Dynamics

3.2.1. Sediment Characteristics

Out of the four study sites in the Westerschelde, the average grain size diameter (Figure 5) was smallest at the most western locations (1E. Zuidgors and 3*S. Paulina*), closest to the mouth of the estuary and largest more

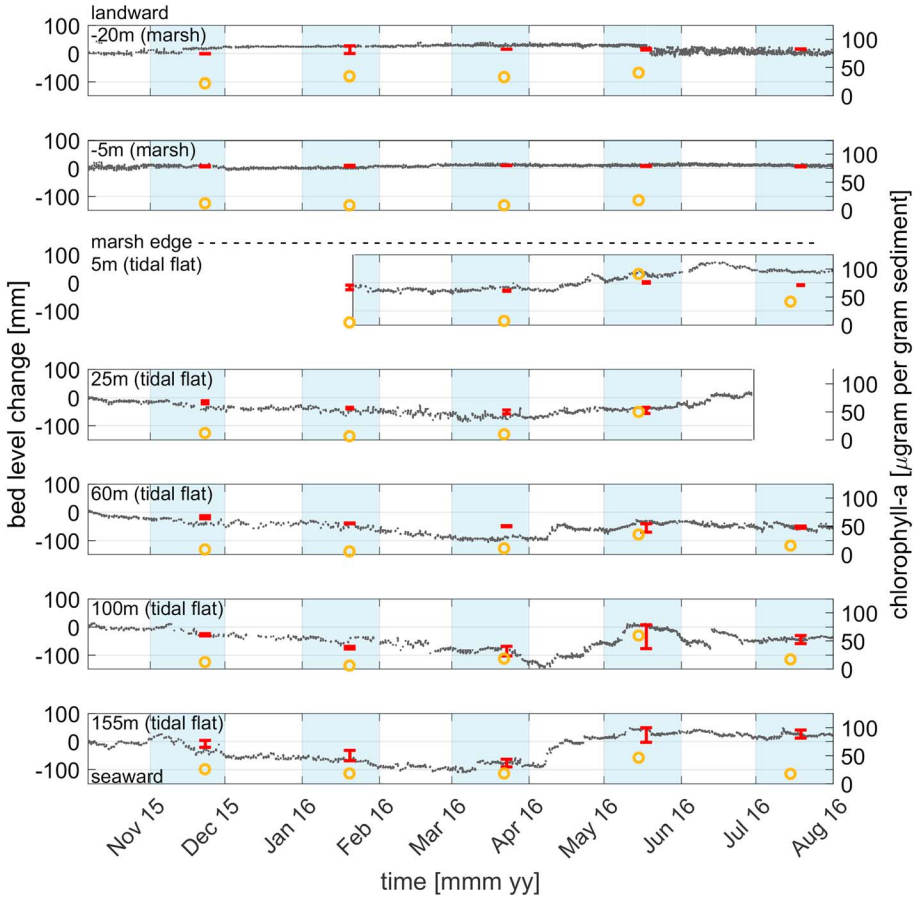

Figure 2. Comparison of obtained bed levels (left *y* axis) using Surface Elevation Dynamic sensors (gray dots) and erosion pins (red bars) with standard deviation, and chlorophyll-*a* levels (yellow markers; right *y* axis) obtained at 1E. Zuidgors. The top panel indicates the most landward position at the transect and the bottom panel the most seaward position. Values at the top left of each panel describe the distance to the marsh edge.

inland (2E. Zimmermanpolder and 4S. Hellegat). There was no general trend over the tidal flat and salt marsh. It was observed that the average grain size was smallest at the most landward location in the salt marsh for the most inland locations (2E. Zimmermanpolder and 4S. Hellegat). The observed average grain sizes at 1E. Zuidgors and 3*S. Paulina* were all in the same range (20–50 μm), no specific differences between the tidal flat and salt marsh were observed (Figure 5). The observed average grain size does not show similar patterns as the patterns observed for bed level change (Figure 4).

3.2.2. Can Waves Explain Bed Level Change?

Measurements of waves at study sites 2E. Zimmermanpolder and 4S. Hellegat, showed that the maximum significant wave height observed per tide, averaged over all obtained tides, at 4S. Hellegat exceeded the values found at 2E. Zimmermanpolder (Figure 6). At both sites waves were higher seaward from the marsh edge and decreased when passing the marsh edge. Waves attenuated further when propagating over the marsh. This pattern was observed for all seasons (Figure 6). At 2E. Zimmermanpolder the maximum significant wave height was higher in winter and lower in summer, while at 4S. Hellegat there was a less distinctive pattern. The highest waves, observed on the tidal flat seaward from the marsh edge at both sites, were related with the largest bed level change (Figure 3 and Figure 6). However, in the marsh, the waves attenuated further, while the bed level change did not show a similar pattern.

Finally at 4S. Hellegat, bed level changes in the marsh were quite similar in spring, fall, and winter, while being lower in the summer (Figure 3). This pattern was not found in the waves observed at the marsh (Figure 6). At 2E. Zimmermanpolder, the pattern of bed level change was less distinctive (Figure 3), while a clear seasonal pattern was identified for the observed waves (Figure 6). At 2E. Zimmermanpolder, bed level changes in fall

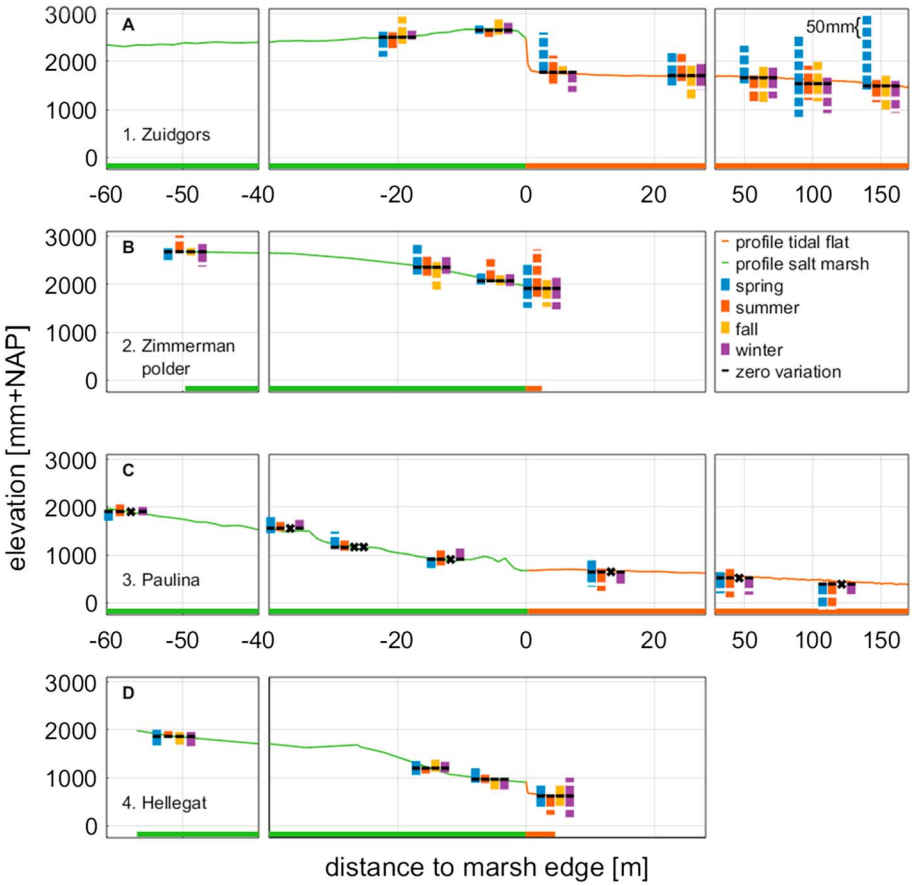

Figure 3. Minimum and maximum bed level change per season for (from top to bottom) 1E. Zuidgors, 2E. Zimmermanpolder, 3S. Paulina, and 4S. Hellegat. The initial bed level profile can be observed by the green (salt marsh) and orange (tidal flat) line. Elevation of the bed level is defined in mm + NAP (i.e., Dutch ordinance level, close to local mean sea level). The bed level changes are shown by four bars, with zero bed level change at the initial bed level profile (black line), maximum sedimentation (bar above the profile), and maximum erosion (bar below the profile). Note that the vertical scale of bed level change differs from the *y* axis scale: A single part of the bar (in between two white lines) is equal to 25-mm change. Missing data for a specific season are indicated with a cross.

were smaller than in summer (Figure 3). The observed patterns for bed level change and waves at 4S. Hellegat were opposite to the patterns at 2E. Zimmermanpolder.

3.2.3. Can Inundation Time Explain Short-Term Bed Level Change?

The tidally averaged inundation time over the entire measurement period (expressed as dry period), closely related to the local elevation, showed a relation with the standard deviation of the bed level change (Figure 7). In general, the bed level change decreased with a decreasing tidal inundation. However, different relationships between bed level change and inundation time were observed at the different transects. Relatively large bed level change with small inundation times appeared at the northern shores (locations 1 and 2, Zuidgors and Zimmermanpolder resp.), while relatively small bed level changes combined with larger inundation times were observed at the southern shores of the Westerschelde (locations 3 and 4, Paulina and Hellegat, respectively). All measurement locations on the marsh were higher, with short inundation times. The tidal flat, located at a lower elevation, had longer inundation times. The interface from tidal flat to marsh was characterized by a cliff at 1E. Zuidgors and 4S. Hellegat, while a smoother transition appeared at 2E. Zimmermanpolder and 3*S. Paulina* (Figure 3).

A distinct pattern was revealed when taking into account all six study sites (Figure 7). A point cloud in this parameter space, representing all measurement locations on the salt marsh and a point cloud representing all measurement locations on the tidal flat, could be dissected by a transition zone. The marsh edge is located in this transition zone. Both dissected point clouds indicate that the location of the lower marsh edge is

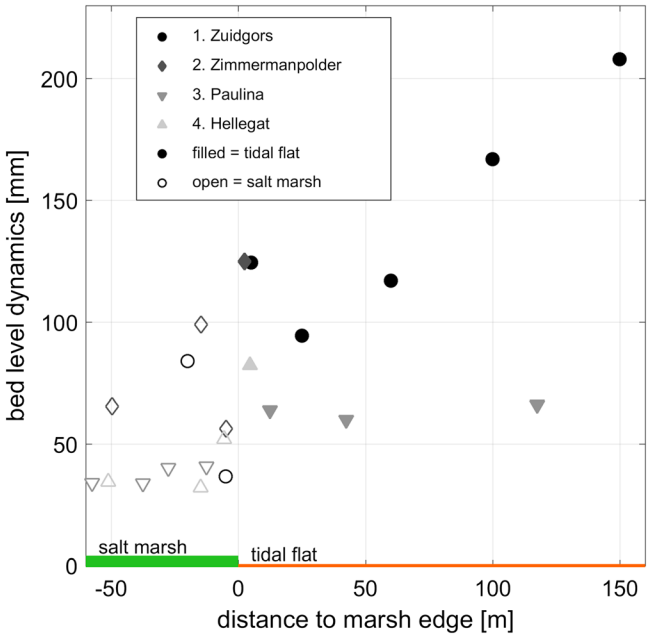

Figure 4. Bed level change (indicated as seasonal maximum obtained bed level change minus seasonal minimum obtained bed level change) per measurement location (indicated by different markers). Bed level change at the marsh is indicated using open markers and with filled markers at the flat.

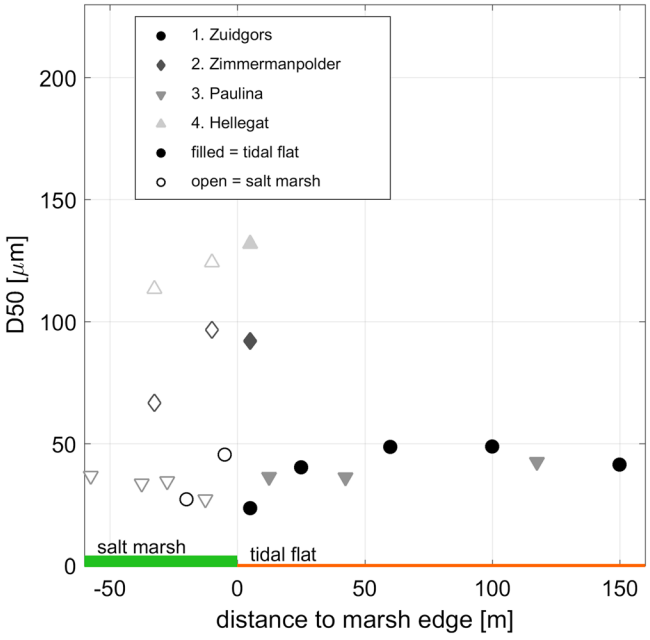

Figure 5. Grain size (D50) measured at the cross-shore transects of the four study sites in the Westerschelde (indicated by different markers). The grain size on the salt marsh is indicated using open markers, and using filled markers at the flat.

restricted by two interacting factors driving plant growth: to withstand longer inundation stress that slows down plant growth, more stable bed levels are required so that plants are not heavily disturbed. Conversely to withstand more dynamic bed level dynamics that disturbs plant growth, lower inundation stress is needed, so that plants grow fast enough to recover from the stress (Figure 7). Thus, as hypothesized in previous studies, inundation time (or dry period), and bed level dynamics are important parameters for vegetation growth and occurrence.

3.2.4. Can Chlorophyll-*a* Explain Short-Term Bed Level Change?

Chlorophyll-*a* levels, obtained at 1E. Zuidgors, increased in Spring (Figure 2, yellow markers). On the tidal flat a clear correlation was observed between the chlorophyll-*a* levels of the sediment—which is a proxy for the presence of microphytobenthos—and bed level change (R^2 is 0.56). Sedimentation was observed in spring, similar to the trend observed in chlorophyll-*a* levels. Chlorophyll-*a* levels of the sediment at the tidal flat and the salt marsh were in the same order of magnitude. In addition, both at the tidal flat and salt marsh, chlorophyll-*a* levels increased in spring (Figure 2). However, on the marsh, bed level change was almost always equal to zero, implying a smaller influence of chlorophyll-*a* of the sediment on bed level change and/or a stabilizing influence of the vegetation cover.

In the period November–January on the tidal flat, both decreasing chlorophyll-*a* level of the sediment and erosion were observed (Figure 2). In the period January–March, the chlorophyll-*a* levels of the sediment slightly increased; however, erosion of the bed was observed. An opposite relation was observed in the period May–July, chlorophyll-*a* levels increased and deposition occurred (Figure 2).

4. Discussion

To obtain a better understanding of the factors constraining the location of the marsh edge and to reveal the role of short-term bed level change in this, bed level change and multiple biophysical parameters were obtained at a range of contrasting sites at the transition between the salt marsh and tidal flat. Combing all measurements across sites showed that the location of the lower marsh edge can be indicated by two interacting factors: inundation time and bed level change. Building on existing knowledge (e.g., Bouma et al., 2016; Hinde, 1954; McKee & Patrick, 1988; Suchrow & Jensen, 2010), our results emphasize that in addition to inundation period, bed level change is an important component in determining the position of the marsh edge.

4.1. Field Data Collection and Processing

Field data were collected at six study sites in the North Sea area. Processed bed level data previously obtained by the SED sensor on the tidal flat at 1E. Zuidgors were validated using sedimentation erosion bars (SEBs), confirming the accuracy of measurements obtained by SED sensors (Hu, Lenting, et al., 2015). The SED sensor and erosion pin measurements obtained at the 1E. Zuidgors salt marsh confirm the applicability of the SED sensor in intertidal vegetated areas. The SED sensor measurements at the tidal flat, obtained in this study, also showed a good correlation with the erosion pin measurements (R^2 = 0.74). The method developed (Appendix A) for converting raw data to bed level data was not capable of detecting a bed level for all obtained measurements, for example, the last (part of

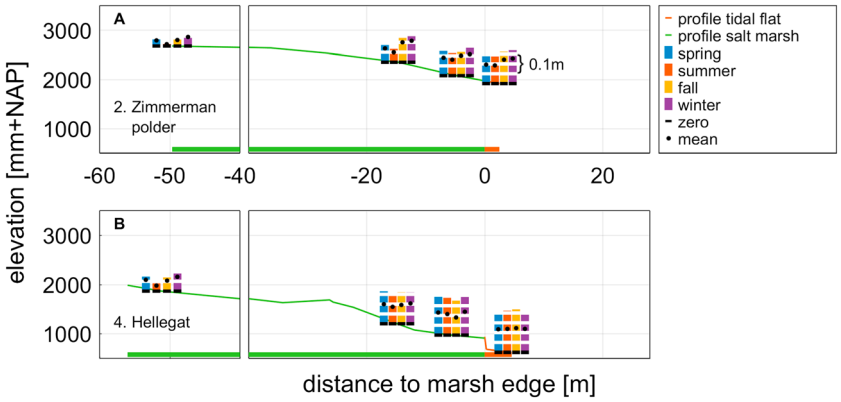

Figure 6. Observed wave heights per season for study site 2E. Zimmermanpolder (a) and 4S. Hellegat (b). The bed level profile is indicated by the green (salt marsh) and orange (tidal flat) line. The observed wave heights are shown by four bars, with no wave height at the bed level profile (black line), and the average wave height per season indicated by a black dot.

September and October) measurements conducted at 1E. Zuidgors did not result in sufficient bed level heights after conversion. However, the obtained bed level changes were comparable with studies wherein similar measurements were conducted (e.g., Hu et al., 2017; Lawler, 2005).

4.2. Toward Understanding Spatial and Temporal Patterns in Short-Term Bed Level Change

In this study we showed that bed level change (both daily and seasonally aggregated) increased from the marsh edge toward the seaward side of the tidal flat. This confirms the findings of earlier studies having spatial data on short-term bed level dynamics (e.g., Bouma et al., 2016; Hu, Wang, et al., 2015). It furthermore agrees with long-term studies (multiple years) that also showed increasing bed level dynamics over the tidal flat toward the sea (e.g., Andersen et al., 2006; Hu et al., 2017; O'Brien et al., 2000). The previously mentioned studies were extended by the present study with measurements at the transition from tidal flat to marsh, resulting in observations both on the vegetated marsh and tidal flat. The seasonal aggregated bed level changes were obtained over multiple contrasting sites, capturing short-term variability per season within longer-term (year) measurements. Seasonality was earlier observed in long-term studies, with in general positive bed level change (sedimentation) in spring and summer and negative bed level change (erosion) in fall and winter (Andersen et al., 2006; O'Brien et al., 2000). This was also observed in this study at the wind-exposed locations at the northern shores in the Westerschelde, but not at the sheltered southern shores in the Westerschelde.

The largest seasonally aggregated bed level change was observed at the locations at the northern shores of the Westerschelde (Figure 3), which are both located perpendicular to the prevailing southwesterly winds (Wang et al., 2017) and hence designated as wind exposed by Callaghan et al. (2010). Location 4S. Hellegat was not designated as exposed, since it is sheltered from the southwesterly winds, but the maximum fetch length at 4S. Hellegat (occurring for westerly winds) was larger than the maximum fetch at the other locations in the Westerschelde (Van der Wal et al., 2008). The differences in fetch also affected the maximum significant wave height (Figure 6), being higher at 4S. Hellegat than at 2E. Zimmermanpolder. The orientation of the study sites in the Westerschelde toward the prevailing wind and the observed hydrodynamics only partly explained the bed level change.

The large accretion at the tidal flats in the Westerschelde, as observed in the spring season, may have been caused by increasing chlorophyll-*a* levels, which is in agreement with earlier observations (Andersen et al., 2005; Austen et al., 1999). In contrast to this ecological control on the tidal flat in spring, it seemed that the ongoing erosive trend in fall and winter (Figure 2) occurred due to the absence of biostabilization, allowing the increasing influence of wind waves. This is supported by earlier observations, where wind waves became more dominant in the winter (Callaghan et al., 2010). The temporally alternating importance of different biological and physical parameters for bed level change shows the complexity of the system wherein the bed level change is influenced by biophysical processes.

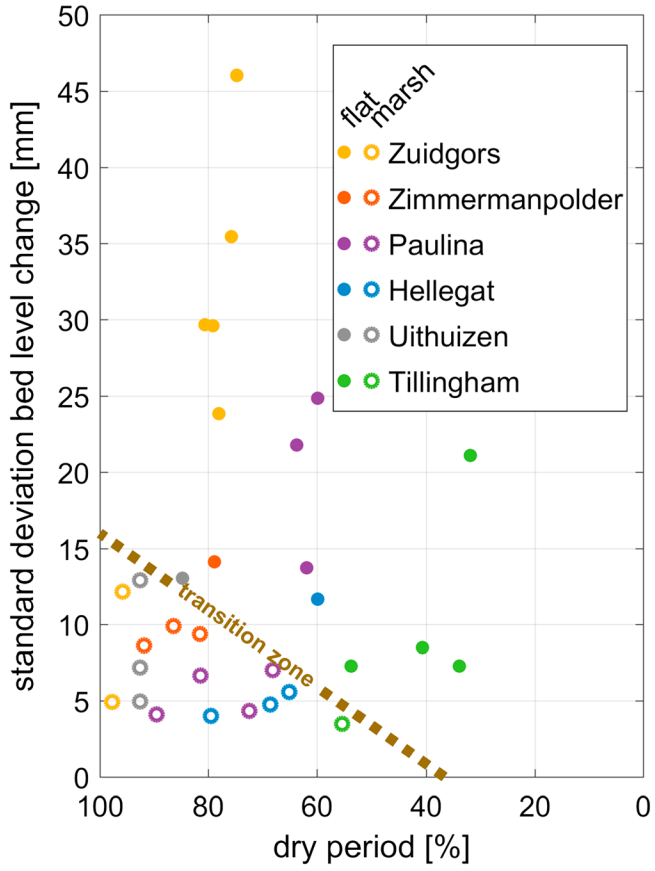

Figure 7. Relation between the standard deviation of the bed level change and average inundation time per measurement transect, being the basis for the location of the tidal flat-marsh transition (transition zone), projected in this parameter space. The measurement locations on the tidal flat (top part) are indicated by a filled marker and indicated with an open marker at the marsh (bottom left part).

In contrast to the highly variable bed levels on the tidal flats, the bed levels remained much more constant on the marshes (Figure 3). Experimental results by Spencer et al. (2016) also showed highly stable bed levels on a marsh during high hydrodynamic energy conditions. Location 2E. Zimmermanpolder seemed like an exception here, having larger seasonally aggregated bed level changes on the marsh than the tidal flat. Perhaps this might be explained by the fact that *Bolboschoenus maritimus* (*Scirpus maritimus*) was the dominant pioneer vegetation type, whereas *Spartina anglica* was the dominant pioneer species at all other locations in the Westerschelde. The higher biomass and stem density of *Spartina* compared to *Scirpus* is apparently associated with a greater sediment stabilizing ability of *Spartina*. In addition to the more variable bed levels on the marsh of 2E. Zimmermanpolder, the maximum significant wave heights (Hm0) on the marsh were more variable both in space and time over the different seasons than at 4S. Hellegat. Finally, the average grain size of the sediment was much coarser at the eastern locations in the Westerschelde (Figure 5), indicating possibly a less cohesive sediment, more vulnerable to erosion. Thus, the incongruous seasonally aggregated bed level changes on the marsh of 2E. Zimmermanpolder may possibly be explained by a different vegetation species, more variable wave heights, and a coarser sediment.

4.3. The Location of the Marsh Edge in Relation to Inundation Stress and Bed Level Change

Over annual to decadal time scales, marsh edge is able to extend seaward and retreat landward (Allen, 2000; Cox et al., 2003; Francalanci et al., 2013; Van der Wal et al., 2008; Wang et al., 2017), affecting the width of the marsh. A narrower marsh width decreases its capacity for wave attenuation (e.g., Vuik et al., 2016), making in-depth understanding of the dynamics driving marsh width key to being able to use marshes for coastal defense (Bouma et al., 2014). At 1E. Zuidgors, marsh edge erosion has been occurring place for decades, and a clear cliff has formed, while at 2E. Zimmermanpolder the *Scirpus* vegetation does not have a marsh cliff, likely because the now retreating Scirpus at the marsh edge was relatively recently (1990s) established. At the southern shores of the Westerschelde a cliff was observed at 4S. Hellegat, but not at 3*S. Paulina*, probably due to the expanding marsh edge here (Van der Wal et al., 2008). It is recommended to measure the lateral dynamics (expansion and erosion) of the marsh edge, possibly with horizontal SED sensors when cliff formation appears, to find possible direct relations with bed level change of the immediate surroundings.

Notwithstanding longer-term controls on decadal marsh edge position changes, daily bed level change, driven by the combination of a number of ecological and physical processes (Corenblit et al., 2011; Deegan et al., 2012; Friedrichs, 2011; Green & Coco, 2014; Mariotti & Fagherazzi, 2010), has been showed to determine the elevation in the tidal prism where seedlings of salt marsh pioneer species can establish seasonally (Bouma et al., 2016; Cao et al., 2018; Silinski et al., 2016). Moreover, bed level change at the tidal flat adjacent to a stable marsh platform has also been identified as a process driving cliff initiation (Bouma et al., 2016). Present results agree with, and extend beyond, Bouma et al. (2016), by showing that across multiple sites, the location of the marsh edge appears to depend on the combined effect of daily bed level changes and inundation period. The latter is closely related to the local elevation (Balke et al., 2016). In case of large daily bed level changes the marsh edge will occur at relative high elevations with little inundation stress. In contrast, at locations with little bed level change, the marsh edge tolerates long inundation and will occur at relative low elevations (Figure 7).

The daily bed level change on the tidal flat may be expected to depend on wave formation, which depends on the tidal-flat elevation relative to mean sea level (Mariotti & Fagherazzi, 2010). The effect of waves observed at the different measurement sites in the present paper mainly showed a relation with the bed

level change at the tidal flat. Waves, as well as bed level changes, were substantially higher than in the marsh. Changes in the tidal prism affecting inundation period and possible bed level change via wave formation have, in the past, resulted in changes from a seaward extending marsh edge to a landward retreating marsh edge (Cox et al., 2003). When distinguishing ship and wind waves, in the Westerschelde no evidence was found to relate the marsh edge growth or retreat to ship waves (Cox et al., 2003).

Present results imply that bed level change and inundation period near the marsh edge can be seen as an indicator for the development of the marsh edge by driving or controlling plant growth. The border between tidal flat and marsh in the parameter space of bed level change and inundation period is thin, indicating the sensitivity to changes. This emphasizes the importance of well-considered anthropogenic interventions in estuaries in the context of salt marsh change and flood protection, since anthropogenic interventions can affect bed level change and the inundation period (Allen, 2000; Cox et al., 2003). Moreover, increasing storm intensity (e.g., Knutson et al., 2010) and sea level rise (Donnelly et al., 2004) in the context of climate change may possibly also affect bed level changes and inundation times at the tidal flat and near the salt marsh edge. This may lead to a shifting marsh edge and thus changes in marsh width.

5. Conclusions

At four study sites in the Westerschelde, the Netherlands, seasonally aggregated bed level changes decreased from the tidal flat toward the marsh edge. The largest positive bed level change (i.e., sedimentation) occurred in spring and the largest negative bed level change (i.e., erosion) was observed in winter. The bed level changes in spring were related to the presence of diatoms (indicated by chlorophyll-*a* levels) at the tidal flat. However, a generic relation between bed level change and differences in hydrodynamics over the seasons was not found. The smallest bed level change (almost negligible) were found in the salt marshes, indicating stability of marshes and their potential for inclusion in coastal defense schemes, given the decreasing wave heights over the marsh toward the landward dike.

Present results from three different tidal basins (four in the Westerschelde, one in the Waddensea, and one in the Thames estuary) suggest that the location of the marsh edge is determined by interactive effects of bed level change and inundation time, which both control plant growth. If bed level change is high, the marsh is observed to occur at higher elevations with lower inundation stress. Conversely, when bed level change is low, the marsh is observed to occur at lower elevations with greater inundation stress. If the present finding is extrapolated, it has major implications for the management of coastal zones (i.e., controlling specific physical processes) if we want to maximize marsh width for flood safety.

Appendix A: Field Data Processing of SED Sensors

The SED sensor collects measurements of the bed level by running a current through the light-sensitive cells, which is transformed into a voltage over a resistor (Hu, Lenting, et al., 2015). In general the voltage output for underground light-sensitive cells is zero, a transition zone to a higher voltage output is showed by the light-sensitive cells around the bed level (Figure A1). Consequently, the raw data typically show a tilted S-shaped curve. The exact shape of the curve may be influenced by factors affecting the light intensity surrounding the SED sensor, like time of day, cloudiness, water level variations, vegetation biomass, and dirt/algae on the sensor. The influence of biological and physical processes on the voltage profile for the different measurement intensities was extensively tested. Experiments were conducted to determine the applicability of the SED sensor surrounded by dense vegetation as well as the applicability with algae and dirt at the transparent cover.

To be able to work well under different light intensities, the SED sensor contains resistors with three different resistances: high, medium, and low. All sensitivities were used to translate measurements obtained under different light intensities into bed level change. The different sensitivities maximize the period measurements can be conducted. The method developed to analyze the raw data from the SED sensor uses the high sensitivity with low light availability (e.g., dusk and dawn). This further elaborates on the method developed by Hu, Lenting, et al. (2015), wherein a threshold for only one sensitivity was used.

Another factor that may influence the level where the sediment-air transition is detected is when scouring holes occur around the SED sensor. Scouring holes may occur when equipment is mounted in the bottom of intertidal area. Scouring holes around SED sensors were only observed around some SED sensors at the

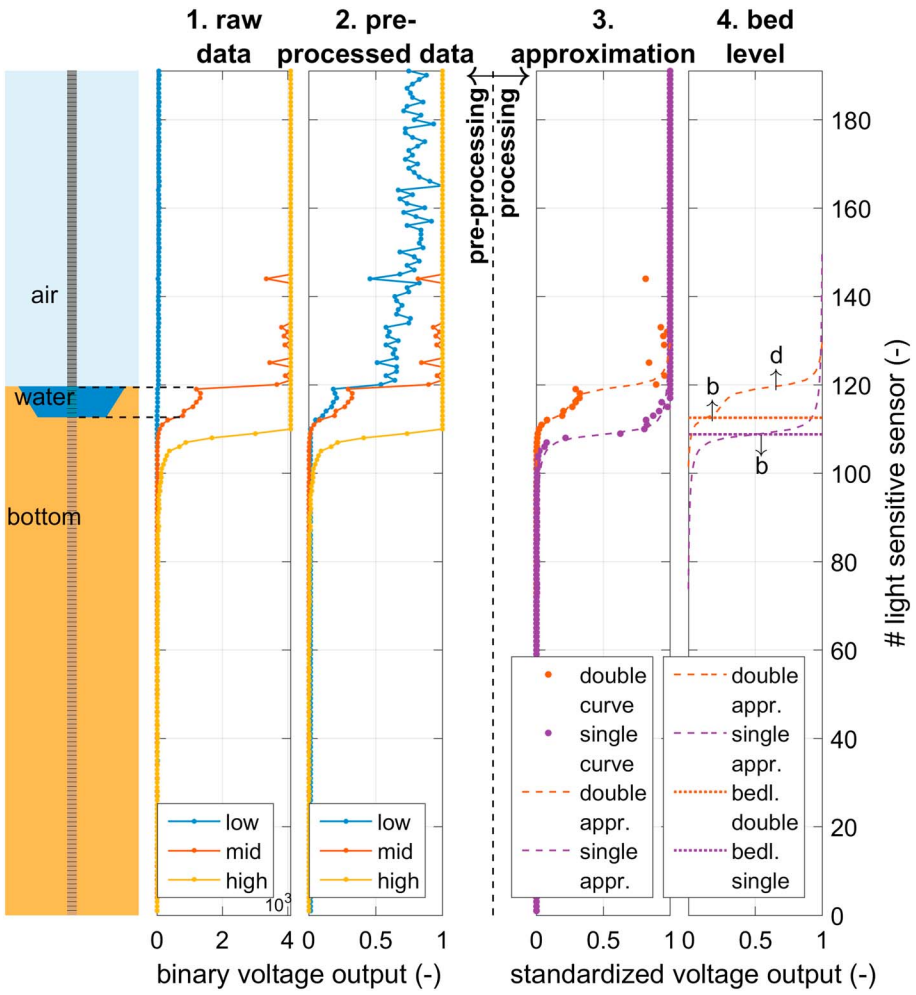

Figure A1. The different steps of (pre)processing the data. A schematic sensor (panel 1), from a measurement at 1E. Zuidgors. The data of the different sensitivities, low (blue), mid (red) and high (blue) is showed in panels 2 (raw) and 3 (preprocessed). The midsensitivity is used to approximate using a double and single arctan function (red and purple, respectively; panel 4). Bed levels were found at parameters *b* and *d* (panel 5).

tidal flat, having a depth of maximum 5 cm. The typically tilted S-curved signal was influenced by the scouring hole, showing two transition zones.

An autonomous script was developed to process the raw data of the measurements, meaning no contextual data representing measurements of, for example, water levels or daytime and nighttime were added. The voltage data obtained by the SED sensor range between 0 and 3.3 V and is scaled to store as 12-bit integers ranging between 0 and 4095. To process the data, the following steps were taken. Before obtaining the bed level, the raw data were preprocessed. The noise was reduced in three steps (Figure A1, panels 2 and 3):

1. To create a consistent profile of all light sensors, the value of the belowground sensors was set to 0, by determining the vertical highest located light sensor with output 0 and forcing all output vertically below this sensor to be 0.
2. The voltage curves were standardized for comparing the different sensitivities within a single time step.
3. The data were filtered per curve using a third-order one-dimensional median filter, to decrease the remaining general noise appearing due to discrepancies between the light-sensitive sensors in the SED sensor.

After preprocessing the raw data, bed levels were obtained by approximating the preprocessed signal with a single (equation (A1)) or double (equation (A2)) arctan function. For a single arctan approximation the bed level was found at parameter *b* (equation (A1) and Figure A1) and for a double arctan approximation the

bed level was found at the minimum of parameters *b* and *d* (equation (A2) and Figure A1). Whether a single or double arctan function was used, depends on the coefficient of determination for measured versus approximated data (R^2). The coefficient of determination was calculated using the sum of squares of residuals (SS_{resid}) and the total sum of squares (SS_{total}; equation (A3)). SS_{resid} is the sum of the squared differences of the measured and predicted value, while SS_{total} is the sum of the squared differences of the measured and the average value. In general, a curve with a single transition zone was approximated best by a single arctan function and a curve with a double transition zone was approximated best by a double arctan function (Figure A1, panels 4 and 5).

$$a * \arctan(x - b) + e \tag{A1}$$

$$a * \arctan(x - b) + c * \arctan(x - d) + e \tag{A2}$$

$$R^2 = 1 - \frac{SS_{resid}}{SS_{total}} \tag{A3}$$

The light resistant cells did not register any light during night time and inundation, because light intensities were too small. So during nighttime and inundation, the voltage output for all light resistance cell was approximately zero, making it impossible to convert the raw data to bed levels.

To reduce the uncertainty of the bed level measurements per time step, measurements were window averaged (window of 6 hr). In order to average the data, isolated measurements per time step (one or two measurements surrounded by time steps without a measurement) were removed.

Possible outliers occurred due to the different vertical locations of the transition zone when comparing voltage curves from the different sensitivities during a single measurement. Differences in voltage curves for the low-, middle-, and high-sensitivity measurement during increasing or decreasing light intensities were probably the cause. However, in this study the small amount of outliers observed were almost all dampened by window averaging the processed data.

Acknowledgments
This work is part of the research program BE SAFE, which is financed by the Netherlands Organization for Scientific Research (NWO) (grant 850.13.010) and part of the EU FP7 project FAST (Foreshore Assessment using Space Technology) (grant 607131). Additional financial support has been provided by Deltares, Boskalis, Van Oord, Rijkswaterstaat, World Wildlife Fund, and HZ University of Applied Science. Bas W. Borsje was supported by the Netherlands Organization for Scientific Research (NWO-STW-VENI; 4363). We acknowledge V. Vuik for providing the wave data, J. de Mey for preliminary work on processing raw data obtained with the SED sensor, and the NIOZ for analyzing the samples in the laboratory and for providing technical assistance. Finally, we acknowledge the useful comments provided the reviewers. Data and scripts in support of this manuscript are available at https://doi.org/10.4121/uuid:c0be318c-9858-4a05-a546-782e29b4abef.

References

Allen, J. R. L. (2000). Morphodynamics of Holocene salt marshes: A review sketch from the Atlantic and Southern North Sea coasts of Europe. *Quaternary Science Reviews*, *19*(12), 1155–1231. https://doi.org/10.1016/S0277-3791(99)00034-7

Andersen, T. J. (2001). Seasonal variation in erodibility of two temperate, microtidal mudflats. *Estuarine, Coastal and Shelf Science*, *53*(1), 1–12. https://doi.org/10.1006/ecss.2001.0790

Andersen, T. J., Lund-Hansen, L. C., Pejrup, M., Jensen, K. T., & Mouritsen, K. N. (2005). Biologically induced differences in erodibility and aggregation of subtidal and intertidal sediments: A possible cause for seasonal changes in sediment deposition. *Journal of Marine Systems*, *55*(3–4), 123–138. https://doi.org/10.1016/j.jmarsys.2004.09.004

Andersen, T. J., Pejrup, M., & Nielsen, A. A. (2006). Long-term and high-resolution measurements of bed level changes in a temperate, microtidal coastal lagoon. *Marine Geology*, *226*(1-2), 115–125. https://doi.org/10.1016/j.margeo.2005.09.016

Arens, S. M., Slings, Q., & de Vries, C. N. (2004). Mobility of a remobilised parabolic dune in Kennemerland, The Netherlands. *Geomorphology*, *59*(1–4), 175–188. https://doi.org/10.1016/j.geomorph.2003.09.014

Austen, I., Andersen, T. J., & Edelvang, K. (1999). The influence of benthic diatoms and invertebrates on the erodibility of an intertidal mudflat, the Danish Wadden Sea. *Estuarine, Coastal and Shelf Science*, *49*(1), 99–111. https://doi.org/10.1006/ecss.1998.0491

Baeyens, W., van Eck, B., Lambert, C., Wollast, R., & Goeyens, L. (1997). General description of the Scheldt estuary. *Hydrobiologia*, *366*(1), 1–14. https://doi.org/10.1023/a:1003164009031

Balke, T., Stock, M., Jensen, K., Bouma, T. J., & Kleyer, M. (2016). A global analysis of the seaward salt marsh extent: The importance of tidal range. *Water Resources Research*, *52*, 3775–3786. https://doi.org/10.1002/2015WR018318

Barbier, E. B., Koch, E. W., Silliman, B. R., Hacker, S. D., Wolanski, E., Primavera, J., et al. (2008). Coastal ecosystem-based management with nonlinear ecological functions and values. *Science*, *319*(5861), 321–323. https://doi.org/10.1126/science.1150349

Borsje, B. W., vanWesenbeeck, B. K., Dekker, F., Paalvast, P., Bouma, T. J., van Katwijk, M. M., & de Vries, M. B. (2011). How ecological engineering can serve in coastal protection. *Ecological Engineering*, *37*(2), 113–122. https://doi.org/10.1016/j.ecoleng.2010.11.027

Bouma, T. J., van Belzen, J., Balke, T., van Dalen, J., Klaassen, P., Hartog, A. M., et al. (2016). Short-term mudflat dynamics drive long-term cyclic salt marsh dynamics. *Limnology and Oceanography*, *61*(6), 2261–2275. https://doi.org/10.1002/lno.10374

Bouma, T. J., van Belzen, J., Balke, T., Zhu, Z., Airoldi, L., Blight, A. J., et al. (2014). Identifying knowledge gaps hampering application of intertidal habitats in coastal protection: Opportunities & steps to take. *Coastal Engineering*, *87*, 147–157. https://doi.org/10.1016/j.coastaleng.2013.11.014

Callaghan, D. P., Bouma, T. J., Klaassen, P., van der Wal, D., Stive, M. J. F., & Herman, P. M. J. (2010). Hydrodynamic forcing on salt-marsh development: Distinguishing the relative importance of waves and tidal flows. *Estuarine, Coastal and Shelf Science*, *89*(1), 73–88. https://doi.org/10.1016/j.ecss.2010.05.013

Cao, H., Zhu, Z., Balke, T., Zhang, L., & Bouma, T. J. (2018). Effects of sediment disturbance regimes on Spartina seedling establishment: Implications for salt marsh creation and restoration. *Limnology and Oceanography*, *63*(2), 647–659. https://doi.org/10.1002/lno.10657

Chmura, G. L., Anisfeld, S. C., Cahoon, D. R., & Lynch, J. C. (2003). Global carbon sequestration in tidal, saline wetland soils. *Global Biogeochemical Cycles*, *17*(4), 1111. https://doi.org/10.1029/2002GB001917

Corenblit, D., Baas, A. C. W., Bornette, G., Darrozes, J., Delmotte, S., Francis, R. A., et al. (2011). Feedbacks between geomorphology and biota controlling Earth surface processes and landforms: A review of foundation concepts and current understandings. *Earth-Science Reviews*, *106*(3–4), 307–331. https://doi.org/10.1016/j.earscirev.2011.03.002

Cox, R., Wadsworth, R. A., & Thomson, A. G. (2003). Long-term changes in salt marsh extent affected by channel deepening in a modified estuary. *Continental Shelf Research*, *23*(17-19), 1833–1846. https://doi.org/10.1016/j.csr.2003.08.002

Damme, S. V., Struyf, E., Maris, T., Ysebaert, T., Dehairs, F., Tackx, M., et al. (2005). Spatial and temporal patterns of water quality along the estuarine salinity gradient of the Scheldt estuary (Belgium and The Netherlands): Results of an integrated monitoring approach. *Hydrobiologia*, *540*(1-3), 29–45. https://doi.org/10.1007/s10750-004-7102-2

Deegan, L. A., Johnson, D. S., Warren, R. S., Peterson, B. J., Fleeger, J. W., Fagherazzi, S., & Wollheim, W. M. (2012). Coastal eutrophication as a driver of salt marsh loss. *Nature*, *490*(7420), 388.https://doi.org/10.1038/nature11533–392.

Dieckmann, R., Osterthun, M., & Partenscky, H. W. (1987). Influence of water-level elevation and tidal range on the sedimentation in a German tidal flat area. *Progress in Oceanography*, *18*(1-4), 151–166. https://doi.org/10.1016/0079-6611(87)90031-0

Donnelly, J. P., Cleary, P., Newby, P., & Ettinger, R. (2004). Coupling instrumental and geological records of sea-level change: Evidence from southern New England of an increase in the rate of sea-level rise in the late 19th century. *Geophysical Research Letters*, *31*, L05203. https://doi.org/10.1029/2003GL018933

Duarte, C. M., Losada, I. J., Hendriks, I. E., Mazarrasa, I., & Marbà, N. (2013). The role of coastal plant communities for climate change mitigation and adaptation. *Nature Climate Change*, *3*(11), 961.https://doi.org/10.1038/nclimate1970–968

Fagherazzi, S. (2014). Coastal processes: Storm-proofing with marshes. *Nature Geoscience*, *7*(10), 701–702. https://doi.org/10.1038/ngeo2262

Francalanci, S., Bendoni, M., Rinaldi, M., & Solari, L. (2013). Ecomorphodynamic evolution of salt marshes: Experimental observations of bank retreat processes. *Geomorphology*, *195*, 53–65. https://doi.org/10.1016/j.geomorph.2013.04.026

Friedrichs, C. T. (2011). *3.06—Tidal flat morphodynamics: A synthesis treatise on estuarine and coastal science* (pp. 137–170). Waltham: Academic Press.

Gedan, K. B., Kirwan, M. L., Wolanski, E., Barbier, E. B., & Silliman, B. R. (2011). The present and future role of coastal wetland vegetation in protecting shorelines: Answering recent challenges to the paradigm. *Climatic Change*, *106*(1), 7–29. https://doi.org/10.1007/s10584-010-0003-7

Grabowski, R. C., Droppo, I. G., & Wharton, G. (2011). Erodibility of cohesive sediment: The importance of sediment properties. *Earth-Science Reviews*, *105*(3-4), 101–120. https://doi.org/10.1016/j.earscirev.2011.01.008

Green, M. O., & Coco, G. (2014). Review of wave-driven sediment resuspension and transport in estuaries. *Reviews of Geophysics*, *52*, 77–117. https://doi.org/10.1002/2013RG000437

Herman, P. M. J., Middelburg, J. J., & Heip, C. H. R. (2001). Benthic community structure and sediment processes on an intertidal flat: Results from the ECOFLAT project. *Continental Shelf Research*, *21*(18-19), 2055–2071. https://doi.org/10.1016/S0278-4343(01)00042-5

Hinde, H. P. (1954). The vertical distribution of salt marsh Phanerogams in relation to tide levels. *Ecological Monographs*, *24*(2), 209–225. https://doi.org/10.2307/1948621

Hu, Z., Lenting, W., van der Wal, D., & Bouma, T. J. (2015). Continuous monitoring bed-level dynamics on an intertidal flat: Introducing novel, stand-alone high-resolution SED-sensors. *Geomorphology*, *245*, 223–230. https://doi.org/10.1016/j.geomorph.2015.05.027

Hu, Z., van Belzen, J., van der Wal, D., Balke, T., Wang, Z. B., Stive, M., & Bouma, T. J. (2015). Windows of opportunity for salt marsh vegetation establishment on bare tidal flats: The importance of temporal and spatial variability in hydrodynamic forcing. *Journal of Geophysical Research: Biogeosciences*, *120*, 1450–1469. https://doi.org/10.1002/2014JG002870

Hu, Z., Wang, Z. B., Zitman, T. J., Stive, M. J. F., & Bouma, T. J. (2015). Predicting long-term and short-term tidal flat morphodynamics using a dynamic equilibrium theory. *Journal of Geophysical Research: Earth Surface*, *120*, 1803–1823. https://doi.org/10.1002/2015JF003486

Hu, Z., Yao, P., van der Wal, D., & Bouma, T. J. (2017). Patterns and drivers of daily bed-level dynamics on two tidal flats with contrasting wave exposure. *Scientific Reports*, *7*(1), 7088. https://doi.org/10.1038/s41598-017-07515-y

Hunt, S., Bryan, K. R., & Mullarney, J. C. (2015). The influence of wind and waves on the existence of stable intertidal morphology in meso-tidal estuaries. *Geomorphology*, *228*, 158–174. https://doi.org/10.1016/j.geomorph.2014.09.001

Irmler, U., Heller, K., Meyer, H., & Reinke, H.-D. (2002). Zonation of ground beetles (Coleoptera: Carabidae) and spiders (Araneida) in salt marshes at the North and the Baltic Sea and the impact of the predicted sea level increase. *Biodiversity and Conservation*, *11*(7), 1129–1147. https://doi.org/10.1023/A:1016018021533

Kirwan, M. L., Temmerman, S., Skeehan, E. E., Guntenspergen, G. R., & Fagherazzi, S. (2016). Overestimation of marsh vulnerability to sea level rise. *Nature Climate Change*, *6*(3), 253–260. https://doi.org/10.1038/nclimate2909

Knutson, T. R., McBride, J. L., Chan, J., Emanuel, K., Holland, G., Landsea, C., et al. (2010). Tropical cyclones and climate change. *Nature Geoscience*, *3*(3), 157–163. https://doi.org/10.1038/ngeo779

Lawler, D. M. (2005). The importance of high-resolution monitoring in erosion and deposition dynamics studies: Examples from estuarine and fluvial systems. *Geomorphology*, *64*(1–2), 1–23. https://doi.org/10.1016/j.geomorph.2004.04.005

Lawler, D. M. (2008). Advances in the continuous monitoring of erosion and deposition dynamics: Developments and applications of the new PEEP-3T system. *Geomorphology*, *93*(1), 17–39. https://doi.org/10.1016/j.geomorph.2006.12.016

Marani, M., D'Alpaos, A., Lanzoni, S., Carniello, L., & Rinaldo, A. (2007). Biologically-controlled multiple equilibria of tidal landforms and the fate of the Venice lagoon. *Geophysical Research Letters*, *34*, L11402. https://doi.org/10.1029/2007GL030178

Mariotti, G., & Fagherazzi, S. (2010). A numerical model for the coupled long-term evolution of salt marshes and tidal flats. *Journal of Geophysical Research*, *115*, F01004. https://doi.org/10.1029/2009JF001326

McKee, K. L., & Patrick, W. H. (1988). The relationship of smooth cordgrass (Spartina alterniflora) to tidal datums: A review. *Estuaries*, *11*(3), 143–151. https://doi.org/10.2307/1351966

Mcowen, C. J., Weatherdon, L. V., Bochove, J.-W. V., Sullivan, E., Blyth, S., Zockler, C., et al. (2017). A global map of saltmarshes. *Biodiversity Data Journal*, *5*, e11764. https://doi.org/10.3897/BDJ.5.e11764

Moller, I., Kudella, M., Rupprecht, F., Spencer, T., Paul, M., van Wesenbeeck, B. K., et al. (2014). Wave attenuation over coastal salt marshes under storm surge conditions. *Nature Geoscience*, *7*(10), 727–731. https://doi.org/10.1038/ngeo2251

Murray, A. B., Knaapen, M. A. F., Tal, M., & Kirwan, M. L. (2008). Biomorphodynamics: Physical-biological feedbacks that shape landscapes. *Water Resources Research*, *44*, W11301. https://doi.org/10.1029/2007WR006410

Nelson, J. L., & Zavaleta, E. S. (2012). Salt marsh as a coastal filter for the oceans: Changes in function with experimental increases in nitrogen loading and sea-level rise. *PLoS One*, *7*(8), e38558. https://doi.org/10.1371/journal.pone.0038558

O'Brien, D. J., Whitehouse, R. J. S., & Cramp, A. (2000). The cyclic development of a macrotidal mudflat on varying timescales. *Continental Shelf Research*, *20*(12-13), 1593–1619. https://doi.org/10.1016/S0278-4343(00)00039-X

Reed, D. J. (1988). Sediment dynamics and deposition in a retreating coastal salt marsh. *Estuarine, Coastal and Shelf Science*, *26*(1), 67–79. https://doi.org/10.1016/0272-7714(88)90012-1

Rupprecht, F., Möller, I., Evans, B., Spencer, T., & Jensen, K. (2015). Biophysical properties of salt marsh canopies — Quantifying plant stem flexibility and above ground biomass. *Coastal Engineering*, *100*, 48–57. https://doi.org/10.1016/j.coastaleng.2015.03.009

Shepard, C. C., Crain, C. M., & Beck, M. W. (2011). The protective role of coastal marshes: A systematic review and meta-analysis. *PLoS One*, *6*(11), e27374. https://doi.org/10.1371/journal.pone.0027374

Silinski, A., van Belzen, J., Fransen, E., Bouma, T. J., Troch, P., Meire, P., & Temmerman, S. (2016). Quantifying critical conditions for seaward expansion of tidal marshes: A transplantation experiment. *Estuarine, Coastal and Shelf Science*, *169*, 227–237. https://doi.org/10.1016/j.ecss.2015.12.012

Singh Chauhan, P. P. (2009). Autocyclic erosion in tidal marshes. *Geomorphology*, *110*(3-4), 45–57. https://doi.org/10.1016/j.geomorph.2009.03.016

Sirvent, J., Desir, G., Gutierrez, M., Sancho, C., & Benito, G. (1997). Erosion rates in badland areas recorded by collectors, erosion pins and profilometer techniques (Ebro Basin, NE-Spain). *Geomorphology*, *18*(2), 61–75. https://doi.org/10.1016/S0169-555X(96)00023-2

Spencer, T., Möller, I., Rupprecht, F., Bouma, T. J., Wesenbeeck, B. K., Kudella, M., et al. (2016). Salt marsh surface survives true-to-scale simulated storm surges. *Earth Surface Processes and Landforms*, *41*(4), 543–552. https://doi.org/10.1002/esp.3867

Staats, N., de Deckere, E. M. G. T., de Winder, B., & Stal, L. J. (2001). Spatial patterns of benthic diatoms, carbohydrates and mud on a tidal flat in the Ems-Dollard estuary. *Hydrobiologia*, *448*(1/3), 107–115.https://doi.org/10.1023/a:1017545204214

Stokes, D. J., Healy, T. R., & Cooke, P. J. (2010). Expansion dynamics of monospecific, temperate mangroves and sedimentation in two Embayments of a barrier-enclosed lagoon, Tauranga harbour, New Zealand. *Journal of Coastal Research*, *261*, 113–122. https://doi.org/10.2112/08-1043.1

Suchrow, S., & Jensen, K. (2010). Plant species responses to an elevational gradient in German North Sea salt marshes. *Wetlands*, *30*(4), 735–746. https://doi.org/10.1007/s13157-010-0073-3

Temmerman, S., Meire, P., Bouma, T. J., Herman, P. M. J., Ysebaert, T., & De Vriend, H. J. (2013). Ecosystem-based coastal defence in the face of global change. *Nature*, *504*(7478), 79–83. https://doi.org/10.1038/nature12859

Van Eerden, M. R., Drent, R. H., Stahl, J., & Bakker, J. P. (2005). Connecting seas: Western Palaearctic continental flyway for water birds in the perspective of changing land use and climate. *Global Change Biology*, *11*(6), 894–908. https://doi.org/10.1111/j.1365-2486.2005.00940.x

Vuik, V., Jonkman, S. N., Borsje, B. W., & Suzuki, T. (2016). Nature-based flood protection: The efficiency of vegetated foreshores for reducing wave loads on coastal dikes. *Coastal Engineering*, *116*, 42–56. https://doi.org/10.1016/j.coastaleng.2016.06.001

Van der Wal, D., Wielemaker-Van den Dool, A., & Herman, P. M. J. (2008). Spatial patterns, rates and mechanisms of saltmarsh cycles (Westerschelde, The Netherlands). *Estuarine, Coastal and Shelf Science*, *76*(2), 357–368. https://doi.org/10.1016/j.ecss.2007.07.017

Wang, H., van der Wal, D., Li, X., van Belzen, J., Herman, P. M. J., Hu, Z., et al. (2017). Zooming in and out: Scale dependence of extrinsic and intrinsic factors affecting salt marsh erosion. *Journal of Geophysical Research: Earth Surface*, *122*, 1455–1470. https://doi.org/10.1002/2016JF004193

Willemsen, P. W. J. M., Horstman, E. M., Borsje, B. W., Friess, D. A., & Dohmen-Janssen, C. M. (2016). Sensitivity of the sediment trapping capacity of an estuarine mangrove forest. *Geomorphology*, *273*, 189–201. https://doi.org/10.1016/j.geomorph.2016.07.038